

Recycling Propellants in Nonpolluting Supercritical Fluids: Novel Computational Chemistry Models For Predicting Effective Solvents

PP-695/E316

FINAL TECHNICAL REPORT

**Betsy M. Rice and Cary F. Chabalowski
U. S. Army Research Laboratory
AMSRL-WM-BD
Aberdeen Proving Ground, Maryland 21005-5066**

PROJECT BACKGROUND

The conventional methods of demilitarization of energetic components of the demilitarization inventory, open burning or open detonation (OB/OD), are being restricted due to the resulting generation of pollution. Additionally, OB/OD destroys valuable energetic materials that could otherwise be reused if extracted from the stockpiles. An alternative demilitarization procedure to OB/OD is supercritical fluid (SF) extraction of the energetic materials. In addition to eliminating pollution, SF extraction allows for the recycling of the recovered ingredients, provided the process is nondestructive. A particularly attractive nondestructive solvent is carbon dioxide, a low-cost environmentally benign solvent with easily accessed critical parameters.

Unfortunately, the ingredients in composite propellants and explosives have varying degrees of solubility in SF CO₂, but it has been observed that solubility is enhanced when trace amounts of simple polar modifiers are added to the SF solvent. Morris et al. [1, 2] reported experimental results on the extraction of RDX from grains of a nitramine-based gun propellant, M43, using SF CO₂ solvents, each of which was modified by one of 34 polar modifiers. This survey study was performed in an attempt to establish correlations between modifier property and increase in the amount of RDX extracted. M43 is composed of 76% RDX, a 16% mix of polymers nitrocellulose and cellulose acetate/butyrate and 8% plasticizer. A grain of M43 has a cylindrical shape and has a mass in the range of 1.2-1.4 g. The grains used in the studies had 19 perforations running axially, and were coated with graphitic glaze. In the first study [1], at the beginning of each extraction (41 MPa, 323.2 K), a single grain, the CO₂ solvent and co-solvent were added to the extraction vessel, and the system allowed to equilibrate for two hours. The extraction vessel was then flushed with neat CO₂. The displaced modified CO₂ solvent was then expanded through a heated flow restrictor into an acetonitrile solvent trap, where any extracted RDX was collected. Increases in the amount of RDX extracted in solvents containing polar modifiers relative to that obtained using neat SF CO₂ were reported as extraction enhancement factors (EEF). The results showed that the most effective modifier is dimethyl sulfoxide (DMSO), with an EEF of 69. Since the removal of RDX was performed through a combined 2-hour static equilibration process followed by a dynamic extraction, it is possible that the solubility limit had not yet been reached. The solubility limit is defined as the mass of a particular solute dissolved in a mass of solvent that has reached thermodynamic equilibrium [1].

In a case in which the solubility limit has not been reached, the EEF due to the addition of polar modifier is assumed to be a relative representation of the enhancement of solubility of a solute due to the modified solvent. Under such an assumption the EEF is probably lower than the enhancement in solubility of a solution in thermodynamic equilibrium. Also, since M43 contains multiple components, it is possible that the amount of RDX extracted is less than that which would be extracted from a sample of pure RDX. In a follow-up study [2], Morris et al. performed dynamic SF extraction of RDX from M43 propellant grains that had been ground. In these measurements, Morris et al. report that the extractions are still probably mass-transfer limited, thus the extraction enhancement ratios most likely underestimate the true solubility enhancement factors. However, Morris et al. report that these measurements are closer to those that would correspond to the solubility limit than those measured using bulk propellant [1]. The amount of RDX extracted in this experiment was greater than that extracted in the study reported in Ref. 1 by factors of ~ 8 for neat CO_2 and ~ 4 for DMSO and acetonitrile modifiers.

Although Morris et al. [1, 2] found weak correlations between modifier properties and increase in EEF due to the addition of polar modifiers, the dependencies of the enhancement factors on the parameters of interest are not established. The objective of this project is to determine, through the use of well-established computational chemistry techniques, the optimal physical conditions and chemical makeup of an effective SF CO_2 solvent with added polar modifier for the extraction of a nitramine explosive. This is accomplished with the development of accurate molecular models for use in computer simulation to determine the conditions that will result in the maximum extraction of reusable ingredients from waste energetic materials. The software developed under this project is designed to allow the non-expert user the ability to easily set up and execute “computer experiments” to determine the conditions associated with optimal extraction for various chemical systems. Additionally, the software can be executed on either Unix-based or Windows-based computer platforms. We have parameterized mathematical models for use in the simulations to describe the 34 co-solvent systems measured in the experimental study [1]; these are included in the software available for distribution. We also performed extensive analyses to understand the enhancement in the solubility of RDX due to the presence of three different polar modifiers in the SF CO_2 solvent. These studies were centered on three representative modifiers whose EEFs spanned the range of the 34 values measured in the experimental study [1]. We studied a modifier with a large EEF, DMSO; one with a moderate EEF, CH_3CN ; and one that had a very small EEF, CH_3OH . We analyzed the dependence on solubility enhancement due to several parameters, such as concentration, dipole moment, temperature and pressure.

The following describes the theory upon which the determination of the solubility of the nitramine explosive in the solvent is based, followed by a description of the models used for the determination, and a discussion of computational methodologies. Results describing simulations in which the potential energy models were assessed and in which solubilities were determined are next described.

Theoretical Formulation for Calculation of the Solubility

When a solute in the solid phase is at equilibrium with a fluid containing the solvent and the solute at temperature T and pressure P , the chemical potential of the solute molecule in the solid phase, μ^S , equals that in the gas (fluid) phase, μ^G :

$$\mu^S(T, P) = \mu^G(T, P). \quad (1)$$

If p^* is the vapor pressure of the solute at temperature T , and if p^* is so small that the vapor at T and p^* can be assumed to be an ideal gas, then one can write

$$\mu^S(T, p^*) = \mu^{\text{ideal gas}}(T, p^*). \quad (2)$$

For the case when the density of the solid phase is assumed to be constant with the variation of pressure from p^* to P at a fixed temperature, one can write

$$\mu^S(T, P) = \mu^S(T, p^*) + \int_{p^*}^P v \, dP = \mu^S(T, p^*) + v(P-p^*), \quad (3)$$

where v is the ratio of the molar volume of the solid and Avogadro's number. The chemical potential $\mu^G(T, P)$ can then be expressed as a sum of two terms: chemical potential, $\mu^{\text{ideal gas}}$, corresponding to the ideal gas at the same temperature and pressure, and the residual chemical potential, μ_r ,

$$\mu^G(T, P) = \mu^{\text{ideal gas}}(T, P) + \mu_r(T, P). \quad (4)$$

Using Eqs.(1)-(4) and the expression [3] for $\mu^{\text{ideal gas}}$ one can obtain

$$N_s/\mathcal{V} = (p^*/kT) \exp(-\mu_r/kT) \exp[v(P-p^*)/kT], \quad (5)$$

where k is the Boltzmann constant and N_s is the number of solute molecules in the solution having volume \mathcal{V} .

By considering N_c to be the number of CO_2 molecules in solution in volume \mathcal{V} , the solubility y can be written as

$$y = N_s/N_c = (p^*/\rho kT) \cdot \exp(-\mu_r/kT) \exp[v(P-p^*)/kT], \quad (6)$$

where $\rho = N_s/\mathcal{V}$, the number density of CO_2 molecules. Equation (6) can be used to compute the solubility using the residual chemical potential, μ_r . The residual chemical potential can be determined using Widom's test particle method [4] in the NPT ensemble for an infinitely dilute solution according to the following formula [5]

$$\mu_r = -kT \ln [\langle V \exp(-\Psi/kT) \rangle / \langle V \rangle]. \quad (7)$$

Here, V is the volume of the fluid, and $\langle \rangle$ denotes the average over all configurations of the fluid and all random orientations of the test particle. Ψ in the above equation gives the total potential energy between a single solute 'test' particle (in the absence of any other solute molecules) and all of the molecules in the solvent for a given configuration. It may be noted that

if density ρ in Eq. (6) represents the number density of solvent (CO_2 +modifier) molecules then y would give the ratio of number of solute molecules to the number of solvent molecules [6, 7].

Computational details of the molecular simulations

(a) NPT-MC simulation of solubility

The simulation cell described herein is composed of n CO_2 molecules and N modifier molecules contained in a cubical box. Periodic boundary conditions are imposed throughout the simulation. The values of n and N have been chosen according to the desired molar concentration $[N/(n+N)]$ of the polar modifier. The total number of solvent molecules ($n+N$) value are ~ 300 , with the exact value dependent on the molar concentration of polar modifier.

We have performed Monte Carlo simulations (MC) in the isothermal-isobaric (NPT) ensemble. The CO_2 molecules are treated as rigid non-spherical bodies, and the method of quaternions [8] is used to represent the orientation of the CO_2 molecules about the centers of mass. One cycle of MC steps consists of $(2n+N+1)$ moves: a random move in the orientation of each of the n CO_2 molecules, $(N+n)$ random translational moves of the centers of mass of all molecules and one random change in the size of the box. For obtaining the residual chemical potential at one value of T and P , 50000-200000 cycles of MC steps have been performed.

A 50% acceptance criterion is used to select the maximum step size. The steps sizes for the box move, the quaternion move, and those of the center of mass moves, are found to be close to 0.30 Å, 0.25, and 0.40 Å, respectively. The cutoff distances for the interaction potentials are equal to one-half the size of the simulation box. Also, the corrections for the long-range interaction potential have been included [8].

(b) Computation of the residual chemical potential

Equation (7) has been used to compute the residual chemical potential, μ_r . It requires the computation of Ψ and V for a large number of random insertions of the test particle over a large number of configurations of the CO_2 + modifier fluid.

In order to compute the potential Ψ for a given configuration of the $(n+N)$ molecules in the box of volume V we first select randomly the location of the test particle (RDX) in the box. We also select randomly the orientation of the point dipole moment associated with the test particle. Ψ is then calculated using the following equation:

$$\Psi = \sum \Psi_k(\text{CO}_2) + \sum \Psi_{ij}(\text{site}) + \sum \Psi_j(\text{dd}) + \Psi(\text{long}). \quad (8)$$

Here $\Psi_k(\text{CO}_2)$ is the interaction potential between the test particle and k th CO_2 molecule, $\Psi_{ij}(\text{site})$ denotes the interaction energy between the test particle and the i th site of the j th modifier molecule, and $\Psi_j(\text{dd})$ gives the dipole-dipole interaction between j th modifier molecule and the test particle [9]. The summation in this equation extends over all molecules and groups

within the cutoff distance R_c from the test particle. $\Psi(\text{long})$ represents the usual long range contribution of the molecules beyond the cutoff distance. The steps used to compute Ψ are described in greater detail in Ref. 11.

C. Calculation of solubility and estimated error

The solubility of RDX in polar-modified CO_2 at supercritical fluid temperatures and pressures has been computed by using Eq. (6) and the residual chemical potential calculated using NPT-MC methods. The partial density ρ of CO_2 that is used in Eq. (6) was determined by averaging the density over all configurations of fluid throughout the MC simulations. The value of v was determined from the experimental density (1.806 g/cc at 300 K) [12] and the volume expansion coefficient ($0.191 \cdot 10^{-3} \text{ K}^{-1}$) [13] of RDX. The values of p^* have been taken from the literature [14, 15]. The enhancement factor in the solubility is defined as the ratio of the computed solubility in the polar-modifier CO_2 solvent to the computed solubility in unmodified CO_2 [10].

The errors due to the finite numbers of Monte Carlo moves and insertions of the test particle procedure were estimated using the procedure described in Ref. 10. This procedure randomly partitions the total data generated in a simulation into two sets, from which averages are calculated and compared. This procedure is repeated hundreds of times for each simulation. The estimated error factor in the solubility is then determined in accordance with the range of variation in the residual chemical potential for 80% of the hundreds of sets so generated. For the solubility results reported in this paper the error factors so estimated are in the range 1.35 to 1.95. The computed results also indicate that the error due to the limited number of insertions of the test particle are smaller than the error due to the finite number of MC moves for all cases. It seems reasonable as the error computed here due to the finite number of MC moves also includes the error due to the finite number of insertions.

Development of the Models

Analytic functions that describe interaction potential energies for chemical systems are parameterized using quantum mechanical (QM) calculations and experimental measurements. Assessments of the quality of the potential energy function is obtained through its subjection to classical molecular simulations [molecular dynamics (MD) or Monte Carlo (MC)]. A QM calculation is based on fundamental first principles, and solution of the QM equations provides a comprehensive and precise description of a system of atoms. The information generated through these calculations is used to develop mathematical models of the chemical system; in this case, the solvent consisting of CO_2 molecules and polar modifier molecules, and the solute molecule. Once these mathematical models are developed, they are then used in classical molecular simulations, from which time-dependent or thermally averaged properties of the material are determined. These simulations allow for the performance of “computer experiments” in which the user can specify the temperature and pressure, and percent concentration of polar modifier in the solvent. Although not first principles, classical molecular simulations using realistic models result in very accurate predictions of reaction dynamics and bulk properties of materials. These calculations are used to determine the solubility of an explosive in SF CO_2 with and without polar modifiers.

Quantum Mechanical Determinations of Intermolecular Interactions

A significant number of quantum mechanical calculations were performed to determine the structural parameters associated with the equilibrium conformation of the molecules in the system and interacting forces between the various pairs of molecules [16-19]. The compilation of this data allowed for the development of the mathematical models that were used in the molecular simulations, discussed hereafter.

Symmetry-Adapted Perturbation Theory (SAPT) was implemented to determine interaction energies between pairs of solute-solvent molecules [16-18]. The focus of our project is on the nitramine explosive RDX; however, it is too large to be effectively treated using the SAPT methodology and thus, a smaller representative chemical system must be used in order to determine the interactions due to the presence of a nitramine explosive. For this purpose, we have selected the small molecule, dimethylnitramine (DMNA). RDX can be thought of as a “trimer” formed by three DMNA molecules arranged in the ring; thus, it is expected that DMNA will have all the required characteristic features of the RDX molecule in terms of interactions with the solvent and cosolvent molecules. Interactions between DMNA with CO₂, CH₃CN, CH₃OH and with another DMNA molecule have been calculated, and analytic functions developed to describe these interactions as functions of internuclear separation and relative molecular orientation [18]. Additionally, similar calculations have been performed to develop CO₂-CO₂ [17] and CH₃CN-CO₂ [16] interaction potentials for use in molecular simulations. For complexes not involving DMNA, the highest available level of SAPT has been applied, while the remaining systems were treated in a more approximate manner due to computational limitations. These calculations indicate that favored interactions between dimer pairs are due to an interplay between electrostatic, dispersion, induction and exchange interactions, none of which can be neglected when considering the shape and stability of a complex. It was found that simple electrostatic arguments for these systems lead to incorrect conclusions about the stabilities of complexes, and that often the dispersion contribution of the interactions between the dimer pairs is as significant as the electrostatic interaction. In general, induction effects are smaller than the other interactions, but in a few cases, they are as large as the dispersion contributions to the energy. If the observations from this work extend to other systems of large molecules (such as biological molecules), then the conventional interpretations of interactions based on the electrostatics alone cannot be trusted as reliable.

A second series of lower-level quantum mechanical calculations were performed for isolated RDX molecules in various conformations, in order to establish the electrostatic potential surrounding the molecules [19, 20]. This information was used to determine atom-centered partial charges that could be used in a standard Coulombic model of electrostatic interactions for RDX with some other molecule. The assignment of the electrostatic charges was made by using the set of atom-centered monopole charges for the isolated molecule (with the structure fixed at the experimental crystallographic configuration) that best reproduces the quantum mechanically derived electrostatic potential. A variety of molecular properties were evaluated using the quantum mechanical information, including vibrational spectra and conformational structures and energies in order to assess the quality of the calculations used in the model development [19].

Interaction Potential Functions for use in Molecular Simulation

RDX/CO₂ systems

As indicated in the earlier section, computational limitations precluded the quantum mechanical description of interactions between pairs of RDX molecules, although insight into the nature of the interactions was obtained through calculation of the DMNA-DMNA interactions. Thus, a functional form for the RDX-RDX interactions was assumed, and the resulting model subjected to a variety of molecular simulations in order to assess its quality. The intermolecular interactions between the molecules of the crystal are approximated using superpositions of pairwise Buckingham (6-exp) (repulsion and dispersion) and Coulombic (C) potentials of the form:

$$V_{\alpha\beta}(r) = A_{\alpha\beta} \exp(-B_{\alpha\beta}r) - C_{\alpha\beta} / r^6, \quad (9)$$

and

$$V_{\alpha\beta}^C(r) = \frac{q_{\alpha} q_{\beta}}{4\pi\epsilon_0 r}, \quad (10)$$

where r is the interatomic distance between atoms α and β , q_{α} and q_{β} are the electrostatic charges on the atoms, and ϵ_0 is the dielectric permittivity constant of space.

The parameters for the 6-exp potential in Eq. (9) were adjusted to reproduce the experimental crystal structure of RDX at ambient conditions, and the partial charges used in the Coulombic interactions [Eq. (10)] were those that reproduced the quantum mechanically derived electrostatic potential surrounding the isolated molecule. The resulting model proved to be extremely accurate in its description of RDX at a large range of temperatures and pressures [20], and also proved to be transferable; that is, it was able to describe a large number of nitramine [21-23] and non-nitramine energetic molecular crystals[24-25]. The results will be described hereafter.

The first model used to describe RDX-CO₂ interactions assumes a potential function $V(R)$ that has a Lennard-Jones form, where R is the separation between molecular centers-of-mass. Its parameters were selected according to the following procedure. A rotationally-averaged interaction potential $V'(R)$ is calculated:

$$V'(R) = \langle \sum_j \sum_k V_{jk}(R_{jk}) \rangle. \quad (11)$$

V_{jk} is the interaction potential between j -th atom of RDX and the k -th atom of the CO₂ molecule, where the atom pairs are separated by a distance R_{jk} and the molecules are arranged relative to one another in an arbitrary orientation. The potential term $V'(R)$ represents the average over a large number ($\sim 5 \times 10^5$) of random relative orientations of RDX and the CO₂ molecule with the centers of mass separated by the distance R_i . The atom-atom interactions in these calculations are represented as Buckingham potentials of the form described in Eq. (9). The parameters A_{jk} ,

B_{jk} , and C_{jk} in the above equation are those used to predict the crystal packing of RDX [20]. For the mixed atomic interactions we have used the arithmetic mean rule for B and the geometric mean rule for the A and C parameters.

We originally selected Lennard-Jones parameters that reproduced the location of the minimum and well depth of the result of Eq. (11); however, solubility predictions using this model were too low by several orders of magnitude compared to the experimental extraction results. We found empirically that a Lennard-Jones potential whose minimum and well depth were shifted from those of $V_i'(R_i)$ by factors of 0.97 and 1.20, respectively, significantly improved the agreement between the calculated and experimental solubility values. The RDX- CO_2 interactions are described by a L-J potential with parameters $\sigma=5.282 \text{ \AA}$ and $\epsilon=0.792 \text{ kcal/mol}$. The $\text{CO}_2\text{-CO}_2$ interactions are described by the Möller-Fischer potential [26].

The following assumptions were made for the description of interactions involving the modifier molecules. In this model a modifier molecule is considered to consist of an ensemble of m groups. For example, for DMSO there are $m=3$ such groups, i.e. CH_3 , CH_3 and SO . Similarly, for CH_3OH and CH_3CN there are two groups ($m=2$), respectively (CH_3 , OH) and (CH_3 , CN). The interaction potential between RDX and a modifier molecule is taken as a sum of the following terms:

$$V_{\text{RDX-M}} = V_{\text{DD}} + \sum V_i(R_i), \quad (12)$$

where V_{DD} is a dipole-dipole interaction term, $V_i(R_i)$ gives the interaction between the RDX molecule and the i -th group of the modifier molecule and R_i is the distance between the centers of mass of RDX and the group. The summation is taken over all m groups of the modifier molecule.

The potential $V_i(R_i)$ has a Lennard-Jones form, and its parameters were selected according to the procedure developed to describe the RDX- CO_2 interaction, described above. In this procedure, a rotationally-averaged interaction potential $V_i'(R_i)$ is calculated:

$$V_i'(R_i) = \left\langle \sum_j \sum_k V_{jk}(R_{jk}) \right\rangle_i. \quad (13)$$

V_{jk} is the interaction potential between j -th atom of RDX and the k -th atom of the group placed at the distance R_{jk} with an arbitrary orientation. The potential term $V_i'(R_i)$ represents the average over a large number ($\sim 5 \times 10^5$) of random relative orientations of RDX and the group with the centers of mass separated by the distance R_i . The atom-atom interactions in these calculations are represented as Buckingham potentials of the form in Eq. (9), and the parameters for these are those used to predict the crystal packing of RDX [20]. For the mixed atomic interactions we have used the arithmetic mean rule for B and the geometric mean rule for the A and C parameters.

For consistency, we have used the same scaling factors to obtain Lennard-Jones parameters to describe the RDX interactions with the groups on the modifier molecules that were

used for the RDX interactions with CO₂. The same parameters were used to describe the CH₃ groups on DMSO, CH₃CN and CH₃OH; however, these were obtained using the results of Eq. (13) for the DMSO interactions with RDX.

For the dipole-dipole interaction term, V_{DD} , we consider that both RDX and the modifier can be considered as point dipoles. In this case, the dipole-dipole interaction is given by an angle-dependent term [9] proportional to $(\mu_a \cdot \mu_b / R^3)$, where μ_a and μ_b denote the dipole moments of RDX and the modifier, respectively, and R gives the distance between the centers of mass of RDX and the modifier.

In describing the CO₂-modifier and modifier-modifier interactions, the molecules are considered to be point masses. The interactions are described by the Lennard-Jones function, with the parameters obtained in the same manner as those obtained for RDX-CO₂, including using the same scaling factors (0.97 for σ and 1.20 for ϵ). Thus this model considers a non-isotropic interaction for each RDX-modifier pair and isotropic interactions for CO₂-modifier and modifier-modifier pairs.

A second model interaction potential was developed to describe the RDX-CO₂ interactions to investigate the effect of assuming a multiple-site model of this interaction (as used for the modifiers). In this model, one center is located on the CO₂ molecule and the RDX molecule has seven sites, each located at the center of mass of its group. The groups consist of the ring, the three NO₂ groups, and the three hydrogen-atom pairs. Parameters were determined in the manner described for the RDX-modifier interactions; however, the scaling factors differ. In this case, the scaling factors for ϵ and σ are 1.55 and 0.88, respectively. This second model will be denoted as the “multisite” model (compared to the previously-described monosite model). Simulations using this model of interactions of RDX-CO₂ were not used in simulations in which polar modifiers were introduced into the solvent.

TNT/CO₂ systems

Two models to describe the interactions between TNT and CO₂ were developed in a manner similar to that for RDX and CO₂: The first assuming a single interaction center on the TNT and CO₂ molecules, respectively, and the second assumes seven sites on the TNT molecule (the ring, the methyl group, the three NO₂ groups, and the two hydrogen atoms) and one on the CO₂ molecule. The monosite interaction potential for TNT with CO₂ requires that the scaling parameters be different from those used in the RDX-CO₂ interaction in order to obtain good agreement with the experimental solubility data.

Results

Numerous computer experiments were performed to assess the quality of the interaction potentials that were developed and to establish the dependencies on the enhancement of solubility due to the composition and nature of the solvent.

Crystalline RDX

This model was developed to achieve modest and narrow goals, i.e. to study the nitramine explosive RDX (1,3,5-hexahydro-1,3,5,-s-triazine) [20]. Isothermal-isobaric molecular dynamics simulations (NPT-MD) and molecular packing calculations (MP) were used to assess the interaction potential through the prediction of the crystal structure of RDX at ambient conditions. The results showed that this model reproduced the crystallographic parameters of RDX to within 2% of experiment in the cell dimensions, with little rotational or translational disorder within the unit cell [20]. Also, we found that this interaction potential could also describe different polymorphic phases of two other nitramine crystals: the polycyclic nitramine 2,4,6,8,10,12-Hexanitrohexaazaisowurtzitane (HNIW, or CL-20) [21] and the monocyclic nitramine Octahydro-1,3,5,7-Tetranitro-1,3,5,7-tetraazacyclooctane (HMX) [22]. Molecular simulations for these crystals predicted cell parameters within a few percent of experiment, and little translational or rotational disorder of the molecules. These successes called for further investigation to determine the limits of the transferability of this interaction potential to other energetic crystals. We performed molecular packing (MP) calculations of 30 nitramine crystals [23]. For most of these crystals, the predicted structural lattice parameters deviate by less than 5% from experiment. Also, for most of the crystals there are small rotations and practically no translations for the molecules in the asymmetric unit cell. The interaction potential was further assessed in molecular packing calculations of 51 crystals containing non-nitramine molecules with functional groups common to energetic materials [24]. MP calculations using this interaction potential reproduced the crystal structures to within 5% of experiment for these 51 non-nitramine systems, including the explosives PETN, nitromethane, TATB, TNT, TNAZ and several nitrocubane derivatives. Also, MD simulations of RDX, HMX, and HNIW under hydrostatic compression produced results that were in good agreement with experiment over the range of pressures investigated experimentally [25]. MD simulations of PETN under hydrostatic compression were in acceptable agreement with experiment up to 5 GPa; beyond that, the disagreement in predictions with experiment was attributed to the inadequacy of the rigid-body approximations imposed in these simulations when applied to floppy molecules. The significance of this effort lies in the ability of the model to predict properties for a wide range of energetic crystals, should such be desired by the user.

RDX solubility in pure SF CO₂

Calculated values of the solubility of RDX in pure SF CO₂ using the monosite and multisite interaction models for the RDX-CO₂ interactions are given in Table 1. Experimental data of Morris [1] are also given for comparison. The general trend in the experimental and computed data at a given temperature is that the solubility increases with pressure. At $P \geq 13.8$ MPa, the solubility exhibits a maximum as a function of temperature. The results for $P > 13.8$ MPa suggest that there may be a maximum in the solubility as a function of temperature beyond the range of temperatures considered in this study. Qualitatively, this behavior is explained by Eq. (6). The solubility is both temperature- and density-dependent directly and indirectly [through its dependence on p^* (which is temperature dependent) and μ_r (which is density dependent)]. As the temperature increases, there is an increase in p^* , which, according to Eq. (6), increases the value of the solubility. At the same time, the density decreases, resulting in a

decrease in the value of $-\mu_r$ and the solubility. Thus, there are competing effects with increasing temperature that could result in a maximum on the solubility vs. temperature curve.

A comparison of the experimental and computed solubilities in Table 1 shows that within the limits of the uncertainties in the computed values, there is very good agreement. Such agreement in the solubility data over the large range of 0.001 to 0.254 mg RDX/g CO₂ is notable, since a small error in the residual chemical potential can lead to a large error in the solubility. The computed results show the same trends in the solubility as functions of temperature and pressure as observed by experiment. For the majority of the points, the agreement between experiment and theory is within a factor of 1.5. The worst agreement corresponds to the solubility at points (338 K, 10.4 MPa) and (323 K, 10.4 MPa) where the experimental solubility values are very low. Computed values by both models are lower than the experimental values.

Table 1. Solubility of RDX in CO₂ as a function of pressure and temperature.

Temp. (K)	Pressure (MPa)	Density (g/cc)	Solubility (mg/g)		
			Multisite	Monosite	Expt. ^{1,2}
353.0	48.3	0.873	0.270	0.257	0.254
	41.4	0.840	0.197	0.178	0.237
	27.6	0.732	0.081	0.171	0.114
	13.8	0.373	0.002	0.003	0.004
338.0	48.3	0.919	0.279	0.166	0.173
	41.4	0.889	0.113	0.192	0.173
	27.6	0.806	0.068	0.113	0.076
	13.8	0.527	0.006	-	0.009
	10.4	0.278	0.0001	0.0001	0.001
323.0	48.3	0.963	0.116	0.193	0.111
	41.4	0.938	0.093	0.092	0.097
	27.6	0.871	0.040	-	0.051
	13.8	0.720	0.011	0.021	0.013
	10.4	0.443	0.0005	0.0003	0.003
308.0	48.3	1.007	0.026	0.005	0.064
	41.4	0.984	0.043	0.026	0.067
	27.6	0.931	0.012	0.040	0.034
	13.8	0.823	0.011	-	0.013
303.0	10.4	0.784	0.009	0.015	0.008
	48.3	1.022	0.037	0.007	0.055
	41.4	1.000	0.025	0.006	0.053
	27.6	0.950	0.023	-	0.032
	13.8	0.867	0.011	-	0.013
	10.4	0.824	0.005	0.009	0.007

A comparison of the results of the two models shows that the results of the monosite model deviate from experiment and results from the multisite model at low temperatures and

high pressures corresponding to high densities of the solvent. The disagreement at high densities is attributed to differences in the interaction potentials for intermolecular separations smaller than 6 Å. For the two models, the interaction potentials between molecular centers are identical for separations greater than these; for smaller separations, the differences are significant.

RDX solubility in polar-modified SF CO₂

We have attempted to identify the molecular properties of representative co-solvents that affect the solubility enhancement of RDX in polar modified SF CO₂. The modifiers, DMSO, CH₃CN and CH₃OH, were chosen to represent very effective, moderately effective, and non-effective co-solvents for solubility enhancement of RDX in SF CO₂. The most obvious distinctions between these modifiers are the molecular sizes and shapes and the magnitude of the dipole moments. The dipole moments of DMSO and CH₃CN (3.96 D and 3.92 D, respectively) are very similar, but nearly twice as large as that of CH₃OH (1.70 D) [27].

(a) Modifier dependence

Table 2 gives the computed solubility results for all three modifiers at T = 323 K and P=41.4 MPa. The solubility enhancement factor (SEF) is the ratio of the solubility of RDX in the polar-modified CO₂ to the value for RDX in pure CO₂ (0.0916 mg RDX/g CO₂ [10]). The SEFs reported in the table show the proper ranking in the effectiveness of the polar modifiers, i.e. DMSO > CH₃CN > CH₃OH compared to the experimental EEFs. The results also qualitatively predict the degree of enhancement as a function of modifier. It is expected that the experimental EEFs would be smaller than the true SEFs due to the experimental procedure and multicomponent nature of the sample used in the experiments. Thus exact agreement between our calculations and experiment would not be expected.

(b) Concentration dependence

Table 2 also shows the variation in the solubility enhancement factor as a function of mole concentration for DMSO and CH₃CN. Figure 1 illustrates this information for DMSO-CO₂ solvents and provides a comparison of the degree of enhancement predicted by theory (upper frame) with that observed in the experimental extractions (lower frame). Although the magnitudes of the enhancements differ between the predictions and experiment, the behavior of the enhancement with increasing modifier concentration is the same. The enhancement factor increases from 14.3 at 2% DMSO mole concentration to 700.6 at 6% DMSO mole concentration. Figure (1) shows that with the increase in concentration there is a rapid (exponential) increase in the enhancement factor followed by a slower increase, suggesting that the limit of saturation is being approached.

We also performed solubility calculations in which the dipole-dipole interaction was set to zero for all concentrations of DMSO reported in Table 2. The calculated enhancement factors were all close to unity, and ranged between 0.65 and 1.57. This indicates that the increase in enhancement factor with increasing concentration is mainly due to the dipole-dipole interaction term. For higher concentrations of the modifier, the model requires a further modification to

account for the rotation of the modifier molecules and a correlation in the directions of the dipole moments of the neighboring molecules.

Table 2. Solubility and solubility enhancement factor (SEF) of RDX due to polar modifiers

Mole Concentration	Partial Density of CO ₂ (g/cc)	Theoretical	Experimental [1,2]	
		SEF	Amount extracted (mg RDX/g CO ₂)	EEF
DMSO				
0.0	0.937	1.0	0.011, ^a 0.08 ^b	
2.0	0.899	14.3		
3.38	0.876	85.9	0.076 ^a	69 ^a
3.5			3.0 ^b	41 ^b
3.99	0.867	176.2		
5.00	0.852	473.0	6.9 ^b	86 ^b
6.00	0.837	700.6		
6.30			9.5 ^b	119 ^b
CH₃CN				
0.0	0.937	1.0	0.011, ^a 0.08 ^b	
3.8			0.98 ^b	12 ^b
3.99	0.835	24.4	0.28 ^a	25 ^a
6.00	0.793	174.7		
6.1			1.3 ^b	16 ^b
CH₃OH				
0.0	0.937	1.0	0.011, ^a 0.08 ^b	
5.54	0.834	2.7		1.4 ^a

a. Static-dynamic extraction on bulk M43 Propellant (Ref. 1)

b. Dynamic extraction on ground M43 Propellant (Ref. 2)

(c) Dipole moment dependence

We have investigated the effect of changing μ_b while keeping all other parameters (including the L-J interaction parameters) unchanged in order to establish the effect of dipole-dipole interactions between RDX and a polar modifier. We performed calculations corresponding to experimental conditions (T=323 K, P=41.4 MPa) for DMSO (3.38%), CH₃CN (3.99%) and CH₃OH (5.54%), but the dipole moment was set to zero for each of the modifiers. The other parameters of the potential were not changed in the simulation. This has the effect of including molecular size and shape, but it precludes electrostatic interactions. The DMSO, CH₃CN and CH₃OH systems have enhancement factors of 1.4, 1.0 and 0.7, respectively, under these

conditions. This suggests that the presence of a dipole moment has a significant effect on solubility enhancement.

We next investigated the variation in the solubility enhancement factor as a function of μ_b for CO₂-DMSO (3.38%) at T=323 K and P=41.4 MPa. The results are given in Table 3 and shown in Fig. 2. These data suggest that the enhancement factor is very sensitive to the magnitude of the dipole moment of the modifier. Figure 2 shows that the increase in the solubility with the increase in the dipole moment of the modifier is nearly exponential. The enhancement factor for a null dipole moment is 1.4 and is 870.3 for a dipole moment equal to 5.0 D. This suggests that the low value of the enhancement factor for the CH₃OH/CO₂ system is due mainly to the small dipole moment (1.70 D).

Table 3. Solubility Enhancement Factor (SEF) as function of modifier dipole moment (3.38% concentration of modifier in CO₂, T=323 K, P=41.4 MPa). All other modifier parameters correspond to DMSO.

μ_b (Debye)	SEF
0.0	1.4
1.0	1.8
2.0	4.0
3.0	15.1
3.96	85.9
5.0	870.3

(d) Comparison of the Enhancement Factors of DMSO and CH₃CN

The preceding discussions indicate that the magnitude of the dipole moment is a significant factor in solubility enhancement, however, it does not account for the total effect. This is evident upon comparison of the performance of DMSO and CH₃CN as polar modifiers. DMSO and CH₃CN have nearly the same values of dipole moment. If the solubility enhancement factor is a function of only the dipole moment of the modifiers, then CH₃CN should have a solubility enhancement factor that is only 5% smaller than DMSO, according to the results shown in Table 3 and Fig. 2. However, the enhancement factors at 3.99% modifier concentration for CH₃CN (24.5) is 86% smaller than that of DMSO (176.2). Clearly, there are additional factors other than dipole moment which affect the solubility. One factor could be the effect on the solvent structure due to the modifier. We will investigate the solvent structure by analyzing energetically favored configurations of the test particle-solvent system and by calculating pair distribution functions for the solvent molecules.

Within these simulations we know that the largest contributors to the value of μ_r are those configurations for which the potential Ψ experienced by the test particle is attractive [Eq. (7)]. Likewise, we know the configurations that do not have a significant contribution to the value of μ_r are those for which $\Psi > 0$, which are typically due to repulsive interactions by close approach of solvent molecules to the test particle. We have extracted from the total those configurations of

the RDX/CO₂-modifier solution that have values of $\Psi < 0$. The number of such configurations is small; for example, in a typical run we found that the number of configurations for which Ψ is attractive ($\Psi < 0$) is 34 million out of a total 250 billion insertions.

We next attempted to quantify the number of modifier molecules in the neighborhood of RDX for the energetically-favored configurations. For this purpose, we considered a modifier molecule to be a neighbor if it is within 7.0 Å distance of the RDX molecule. Figure 3 shows the average number of DMSO neighbors of a RDX molecule as a function of Ψ for fluid configurations at $T = 323$ K, $P=41.4$ MPa, and DMSO concentration 6%. The figure shows that lowest-energy configurations are those for which there are more than one modifier in the neighborhood of the RDX particle. The behavior of the curve suggests a preference of RDX for occupying a site that has three or more modifier molecules as its neighbors.

The pair distribution function $g(R)$ for CO₂-CO₂, DMSO-DMSO and DMSO-CO₂ for CO₂ with 3.38% DMSO at $P=41.4$ MPa and $T=323$ K were calculated, and shown in the upper frame of Fig. 4. The corresponding curves for CO₂-CH₃CN (3.99%) and CO₂-CH₃OH (5.54%) at the same P and T are shown in the middle and lower frames of Fig. 4, respectively. The leading peak for CO₂-CO₂ in all the three curves is located at 4.05 ± 0.05 Å. The location of the leading peaks for the CO₂-modifier and modifier-modifier pair distribution functions varies with the modifier. The location of the leading peak is 5 to 9% larger than the corresponding value of σ parameter of L-J interaction. The locations of these peaks are insensitive to the modifier concentration, temperature and pressure in the range of these studies. These figures show that CH₃CN-CH₃CN intermolecular separations are about 12% smaller than the DMSO-DMSO separations. This is consistent with the 10% higher value of the sigma parameter for the DMSO-DMSO interactions than that for CH₃CN-CH₃CN. According to the arithmetic mean rule for the sigma parameter, a 10% difference in the modifier-modifier interactions would result in a 5% difference in the effective sizes of RDX-CH₃CN and RDX-DMSO.

The difference in the RDX-CH₃CN and RDX-DMSO interactions can also be understood from Fig. 5. Figure 5 shows the interaction potential given by Eq. (12) between RDX and a modifier molecule as a function of the distance R between their centers of mass in the most favorable orientation. The most favorable orientation is defined here as the orientation of the modifier molecule relative to RDX such that the directions of the dipole moment vectors are antiparallel and the potential given by Eq. (12) is the minimum of all values obtained for 10^5 random relative orientations of the pair for a given value of R .

Figure 5 shows that the value of the well-depth of such a potential, denoted as $V(\text{min.})$, is 6.655 kcal/mole at $R = 5.38$ Å for the DMSO-RDX system. The well-depth of $V(\text{min.})$ for the CH₃CN-RDX system is 6.385 kcal/mole at $R=5.14$ Å. As expected, the effective size parameter for the RDX-DMSO interaction is larger by about 5%. Also, the effective interaction strength is larger for the RDX-DMSO pair by ~ 0.27 kcal/mole. This difference in the interaction strength is one of the important factors for the higher solubility of RDX in DMSO. Additionally, the size difference could explain why RDX is less soluble in CH₃CN. We illustrate this proposal using Fig. 6. The three circles in the left-hand portion of this figure depict three DMSO molecules that surround the RDX molecule. This is a simple two-dimensional representation of a low-energy

fluid configuration determined earlier (energetically favored configurations are those in which three or more modifiers are in the neighborhood of RDX). The four molecules may or may not lie in the same plane. The solid lines connecting the modifier molecules represent the most probable distances between DMSO-DMSO molecules.

The right-hand-side of the figure represents the CH₃CN-RDX analog. The three circles at each apex of the triangle connected by solid lines represent separations that are 12% smaller than those of the DMSO system. This is the same difference in the molecular separations that were determined from the radial distribution functions in Fig. 5. As discussed in preceding paragraphs, however, we estimated that the energetically-favored CH₃CN-RDX distances are only 5% smaller than the DMSO-RDX distances, not 12% smaller. Therefore an RDX molecule inserted into a region in which it was surrounded by three CH₃CN molecules would have a higher probability of experiencing a repulsive interaction than if it was surrounded by three DMSO molecules in a CO₂-DMSO solvent. The increased number of repulsive states sampled in a simulation results in a lower solubility. Repulsive interactions can be avoided if the test particle is inserted at a location that is a sufficient distance from the three modifier molecules. Such an arrangement may provide a non-negligible contribution to the average in Eq. (7). However, the RDX test particle may experience repulsions from other CH₃CN molecules in the solution. Therefore, the test particle samples more energetically unfavorable sites in a CO₂/CH₃CN solution than in a CO₂/DMSO solution. This explanation suggests that in an experiment, the number of arrangements of RDX surrounded by a modifiers at molecular separations that give the optimal attraction for both modifier-modifier and RDX-modifier interactions is smaller for CH₃CN than DMSO, hence the lower solubility. To summarize: Although the dipole moments of CH₃CN and DMSO are nearly same, their contributions to solubility enhancements of RDX at the P, T, and concentration of our studies are different because of the difference in (1) RDX-modifier interaction strength and (2) the size of the modifiers.

(e) Dependence on temperature and pressure

The computed solubility of RDX in CO₂-DMSO (3.38%) as a function of temperature and pressure for a few typical values of P and T are reported in Table 4. The solubility enhancement factors relative to the computed solubility values in pure CO₂ [10] have also been reported in the table. The results show that the solubility increases with the pressure. A comparison of the solubility of RDX in CO₂ with and without [10] modifier shows that the solubility of RDX in polar-modified CO₂ is less sensitive to temperature.

Table 4. Solubility and Solubility Enhancement Factor (SEF) of RDX in CO₂ with 3.38% mole concentration of DMSO as a function of temperature and pressure

T (K)	P (MPa)	Partial Density of CO ₂ (g/cc)	Solubility (mg RDX/g CO ₂)	SEF
323.0	13.8	0.698	0.833	39.4
	41.4	0.876	7.868	85.9
	48.3	0.900	10.654	55.2
338.0	41.4	0.836	9.046	47.1
	48.3	0.863	12.315	74.2
353.0	41.4	0.794	7.419	41.7
	48.3	0.823	9.462	37.0

(f) Other models

We also calculated the solubility at the temperature and pressure given in Table 2 for all three modifiers using models that treat each modifier molecule as a point mass, i.e., taking $m=1$ in Eq. (12). In this model, all potential energy features, including the random selection of directions of dipole moment vectors, are determined by the same procedure described earlier. For purposes of discussion, this model will be denoted as “Model B”, whereas the model described in the earlier sections will be denoted as “Model A”. The calculated enhancement factors for Model B are 1.7, 6.2 and 0.7, for DMSO(3.38%), CH₃CN(3.99%), and CH₃OH(5.54%). The inability of this model to qualitatively reproduce the behavior of experimental EEf may be due to either the inappropriate selection of potential scaling parameters (0.97, 1.20 for σ and ϵ , respectively) or to the failure of the description of RDX-modifier interaction by the sum of a single L-J potential term and a dipole-dipole interaction term.

A third model, denoted “Model C”, assumes modifier-modifier and CO₂-modifier interactions that are different from those of Model A. The CO₂-modifier and modifier-modifier interactions in Model C require that each modifier have m interaction sites, similar to the requirements for the RDX-modifier interactions as described earlier. Use of this model in the NPT-MC generation of solvent configurations does not allow random assignment of the dipole moment of the modifier molecule, as described in simulations using Model A.

The enhancement factors calculated using Model C are found to be very low. The predicted enhancement factor for CO₂ with 3.38% DMSO, T=323 K, P=41.4 MPa is 0.7. We have repeated calculations using Model C for different sets of potential scaling parameters (ranging from 0.97 to 1.35 for σ and from 0.80 to 1.20 for ϵ) for the CO₂-modifier and modifier-modifier potentials such that the densities of the fluid using these different potential scaling parameters are almost the same as that given in Table 2 by Model A. However, the enhancement factors were very low in all cases. Further, solubilities predicted using Model C show a weak dependence on dipole moment, e.g., the enhancement factor varies from 0.4 to 1.9 as the dipole

moment of the modifier is varied from 0.0 to 6.0 D, while keeping all other parameters the same as that for DMSO.

We think the differences in behavior between Model C and Model A can be attributed to the following: In Model C, the configurations corresponding to the lowest enthalpy values are those in which the dipole moments of adjacent modifier molecules are aligned in an antiparallel orientation. In such a configuration, the dipole-dipole interaction between the test particle (RDX) and a modifier neighbor would tend to cancel the dipole-dipole interaction between the RDX and the adjacent modifier neighbor whose dipole is in the antiparallel orientation. Such a cancellation would lead to the lower contribution to the solubility. In Model A, on the other hand, the orientations of the dipole moments are chosen randomly. Hence the random selection of the direction of the dipole moments of two modifier neighbors may, in many cases, have favorable orientations for which the RDX-modifier dipole-dipole interactions are not cancelled.

At a first glance, Model C appears to be more physically representative of the actual fluid than Model A. However, if we consider continuous thermal rotations of the molecules in the real fluid, then we may find that the modifier molecules rotate with different frequencies and as such the relative orientations of dipole moment vectors of the two modifier molecules may frequently become parallel and antiparallel. Since the method of predicting solubility used in this work does not directly allow for the simulation of a dynamic event, such as thermal rotation, it is possible that this dynamic effect is indirectly included in this model using the random selection in Model A. In NPT-MC simulations using Model C, this dynamic reorientation of the dipoles is not incorporated. Thus in Model C the term $\langle V \exp(-\Psi/kT) \rangle$ in Eq. (7) misses the dominant contributions of those states of the solvent in which the dipole moment vectors of the modifiers in the neighborhood of the test particle are nearly parallel to each other and antiparallel to that of RDX. This would explain the success of Model A in the comparison of its predictions to those of Model C.

(g) Limitations of the infinite dilution approximation:

The solubility of RDX in pure CO₂ at T=323 K, P=41.4 MPa (0.0916 mg RDX/g CO₂) corresponds to 1 molecule of RDX in about 55000 molecules of CO₂. Such a solution can reasonably be considered one with infinite dilution. The theoretical method used here is invalid when the solution is not an infinitely dilute solution. The calculated values of the solubility of RDX in pure CO₂ indicate that for those simulations, the infinite dilution assumption is valid. In the present calculations, in which we consider about 300 molecules of solvent in the box, the solubility is less than 1 molecule of RDX in 300 molecules of CO₂ for SEFs up to 180 at this temperature and pressure. Beyond this range, in the finite dilution case, one would require a simulation in the presence of RDX molecules and the (n+N) CO₂ and modifier molecules. This may alter the environment for the test particle. The presence of the RDX molecules at the low-energy-sites in the proximity of a few modifier molecules may prohibit sampling of such favorable sites by the test particle, and the test particle may sample a larger number of repulsive locations than in a solution that does not contain RDX. These conditions would lead to the lower value of solubility than that given by the infinite dilution approximation.

In view of the foregoing discussion it is very likely that the results for DMSO at the 5% and 6% concentrations as reported in Table 2 give an upper limit to the solubility, i.e., it is likely that at these concentrations, lower solubilities than those given in Table 2 will result from calculations using an improved formulation that does not assume the infinite dilution approximation.

TNT solubility in pure SF CO₂

The solubility of TNT in pure SF CO₂ using both monosite and multisite models of the interactions between TNT and CO₂ as a function of temperature and pressure have been performed, and are reported with the experimental values in Table 5. The values of solubility (both experimental and theoretical) are very large compared to those of RDX. The basis for the differences in magnitude of solubilities between the two systems lies in the value of p^* used in Eq. (6). For example, at T=323 K, P=41.4 MPa, the ratio of the computed solubility of TNT and RDX is 333, whereas the corresponding ratio of p^* is 873; at T=308 K, P=13.8 MPa, these two ratios are 827 and 1232, respectively.

Table 5: Solubility of TNT in SCF CO₂

Temp. (K)	Pressure (MPa)	Density (g/cc)	Solubility (mg/g)		
			Multisite	Monosite	Expt ^{(a),(b)}
353.0	27.6	0.732	42.1	29.2	19.4 ^(b)
	13.8	0.373	1.0	-	
338.0	27.6	0.806	37.2	28.5	19.8 ^(b)
	13.8	0.527	3.0	-	
	10.4	0.278	0.1	-	
323.0	41.4	0.938	31.0	44.2	45.6 ^(b)
	27.6	0.871	22.9	23.0	19.4 ^(b)
	13.8	0.720	8.0	-	
	10.4	0.443	1.0	-	
308.0	48.3	1.007	26.1	37.6	50.6 ^(b)
	41.4	0.984	22.4	21.4	34.8 ^(b)
	27.6	0.931	20.2	15.5	18.4 ^(b)
	13.8	0.823	9.1	5.7	9.6 ^(a)
	10.4	0.784	7.8		
303.0	48.3	1.022	22.2	25.3	39.6 ^(b)
	41.4	1.000	31.6	15.5	32.3 ^(b)
	27.6	0.950	22.2	13.8	17.9 ^(b)
	13.8	0.867	12.0		
	10.4	0.824	5.9		
293.0	6.9	0.720	5.3		
	37.9	1.022	9.6	15.3	13.3 ^(a)
	13.8	0.924	8.3	4.3	4.9 ^(a)

(a). Ref. (28)

(b). Results of Ref. (29) has been further analyzed by Morris and are listed in Ref.(28).

The computed solubility of TNT at 353 K, 27.6 MPa corresponds to ~ 2 molecules of TNT in the simulation box containing 216 molecules of CO₂. This suggests that the infinite dilution approximation assumed in the formulated used for these calculations is not valid at this temperature and pressure for the TNT system. For more accurate results at this temperature and pressure, we are required to modify the model by assuming the solvent consists of (n+N) molecules, where n denotes a small number of TNT molecules and N denotes the number of CO₂ molecules. With this consideration, the interaction of the test particle with these n+N molecules should be computed to evaluate Ψ in Eq. (7). By repeating the calculation for different values of n, we can find n such that the computed solubility corresponds to the ratio n/N. The solubility computed in this fashion would not be based on the infinite dilution approximation and as such would be more accurate. For most of the data for TNT reported in Table 5, however, the solubility corresponds to $n \ll 1$; as such, the infinite dilution approximation is expected to be valid for all such computations.

Conclusions

Models for use in molecular simulation of crystalline explosives and explosives in pure and polar-modified SF CO₂ were developed. Simulations were performed to assess the quality of the models, with the results indicating that a significant capacity for predictions using these models exists. Dependence of solubility enhancement factors due to modifier type, dipole moment, concentration, effective size, temperature and pressure were examined. The results suggest that the degree of solubility enhancement has a cooperative dependence on the magnitude of the dipole moment, the number of modifier molecules surrounding the solute particles, and the effective size and strength of the modifier-solute interaction.

SUMMARY OF THE FINAL PRODUCT/DELIVERABLE

The finished product of PP-695 consists of a set of FORTRAN 77 computer codes that predict the solubility of a nitramine explosive in neat or polar-modified CO₂. The working equations for the predictions are based on classical statistical mechanical theories, and the models are developed using the fundamental quantum mechanical theories. Computer simulations using these codes provide a prediction of the solubility of an ingredient of a propellant as a function of the conditions of a proposed experiment, i.e. the temperature, pressure, and percent cosolvent (if desired). The software is available for electronic distribution through the SERDP Support office or by contacting Dr. Betsy M. Rice (phone: 410-306-1904, e-mail: betsyr@arl.mil).

References

1. J. B. Morris, M. A. Schroeder, R. A. Pesce-Rodriguez, K. L. McNesby, and R. A. Fifer, ARL-TR-885, October 1995.
2. J. B. Morris, Proceedings of 1999 JANNAF Safety & Environmental Protection Subcommittee Meeting, CPIA Pub. TBD, April 1999.
3. A. Ben-Naim, *Water and Aqueous Solutions*, (Plenum Press, New York, 1974).
4. B. Widom, *J.Chem.Phys.*, 39 (1963) 2808-2812.
5. K. S. Shing, and S. T. Chung, *J. Phys. Chem.* 91 (1987) 1674-1681.
6. Y. Koga, Y. Iwai, M. Yamamoto, and Y. Arai, *Fluid Phase Equil.* 131 (1997) 83-96.
7. Y. Iwai, Y. Mori, Y. Koga, Y. Arai, and H. Eya, *J. Chem. Eng. of Japan*, 27 (1994) 334-339.
8. M. P. Allen and D. J. Tildesley, *Computer Simulation of Liquids*, (Oxford Science Publications, Oxford, 1993).
9. J. O. Hirschfelder, C. F. Curtiss, and R. B. Bird, *Molecular Theory of Gases and Liquids*, (John Wiley, New York, 1964) p. 851
10. P. M. Agrawal, D. C. Sorescu, B. M. Rice and D. L. Thompson, *Fluid Phase Equilibria*, (1999) 155, 177.
11. P. M. Agrawal, B. M. Rice, D. C. Sorescu and D. L. Thompson, *Fluid Phase Equilibria*, accepted for publication, in press.
12. C. S. Choi and E. Prince, *Acta Crystallogr.* B28 (1972) 2857-2862.
13. M. Dobratz, *Properties of Chemical Explosives and Explosive Simulants*; Lawrence Livermore National Laboratory, Livermore, CA, Report UCRL-52997, 1981; pp.19-131, 19132.
14. J. B. Morris, *J. Chem. Eng. Data*, 43 (1998) 269-273.
15. B. C. Dionne, D. P. Rounbehler, E. K. Achter, J. R. Hobbs and D. H. Fine, *J. Energetic Materials*, 4 (1986) 447-472.
16. P. M. Agrawal, D. C. Sorescu, B. M. Rice and D. L. Thompson, *Fluid Phase Equilibria*, Vol. 155, p. 177 (1999).
17. H. L. Williams, B. M. Rice and C. F. Chabalowski, *Journal of Physical Chemistry A*, Vol. 102, 6981 (1998).

18. R. Bukowski, J. Sadlej, B. Jeziorski, P. Jankowski, K. Szalewicz, S. Kucharski, H. L. Williams and B. M. Rice, *Journal of Chemical Physics*, Vol. 110, p. 3785 (1999).
19. R. Bukowski, K. Szalewicz, and C. F. Chabalowski, *Journal of Physical Chemistry A*, Vol. 103, 7322 (1999).
20. B. M. Rice and C. F. Chabalowski, *Journal of Physical Chemistry A*, Vol. 101, 8720 (1997).
21. D. C. Sorescu, B. M. Rice and D. L. Thompson, *J. Phys. Chem. B* 101 (1997) 798-808.
22. D. C. Sorescu, B. M. Rice and D. L. Thompson, *Journal of Physical Chemistry B*, Vol. 102, 948 (1998).
23. D. C. Sorescu, B. M. Rice and D. L. Thompson, *Journal of Physical Chemistry B*, Vol. 102, 6692 (1998).
24. D. C. Sorescu, B. M. Rice and D. L. Thompson, *Journal of Physical Chemistry, A*, Vol. 102, 8386 (1998).
25. D. C. Sorescu, B. M. Rice and D. L. Thompson, *Journal of Physical Chemistry A* Vol. 103, p 989 (1999).
26. D. C. Sorescu, B. M. Rice and D. L. Thompson, *Journal of Physical Chemistry*, Vol 103, p. 6783 (1999).
27. D. Möller and J. Fischer, *Fluid Phase Equil.*, 100(1994)35-61.
28. D. R. Lide, Ed., *CRC Handbook of Chemistry and Physics*, 74th ed.; CRC Press, Inc.: Boca Raton, FL, 1994.
29. J. B. Morris, Army Research Laboratory, USA, Report No. ARL-TR-1343, 1997.
30. U. Teipel, P. Gerber and H. H. Krause, *Propellants, Explosives, Pyrotechnics* 23 (1998), 82-85.

Figure Captions

Fig. 1: The solubility enhancement factor (SEF) and extraction enhancement factor (EEF) in solvent for $P=41.4$ MPa, $T=323$ K.

Fig. 2: The solubility enhancement factor dependence on the dipole moment μ_b with all other parameters the same as those used for DMSO simulations [$P=41.4$ MPa, $T=323$ K, 3.38%].

Fig. 3: The average number of modifier neighbors of the RDX molecule as a function of the potential, Ψ in kcal/mol, experienced by the RDX molecule as a test particle [$T=323$ K, $P=41.4$ MPa, 6% DMSO].

Fig. 4: The pair distribution function for solvent particles in polar-modified CO_2 solvents at $P=41.4$ MPa, $T=323$ K. Upper frame denotes solvent with a concentration of DMSO=3.38%; middle frame denotes the solvent with a CH_3CN concentration of 3.99%; and lower frame denotes the solvent with a CH_3OH concentration of 5.54%.

Fig. 5: Energetically-favored interaction potential $V(\text{min.})$ (see text) as a function of the distance (in \AA) between the centers of mass of modifier and RDX molecules. DMSO-RDX and CH_3CN -RDX interactions are represented with circles and triangles, respectively.

Fig. 6: Two-dimensional illustration of three modifiers surrounding RDX for the DMSO/ CO_2 system (left-hand portion of the figure) and $\text{CH}_3\text{CN}/\text{CO}_2$ system (right-hand portion of the figure). Solid lines connecting the molecules denote most probable intermolecular separations (determined through computer simulation in the case of modifier-modifier separations and using standard arithmetic mean rules for RDX-modifier separations).

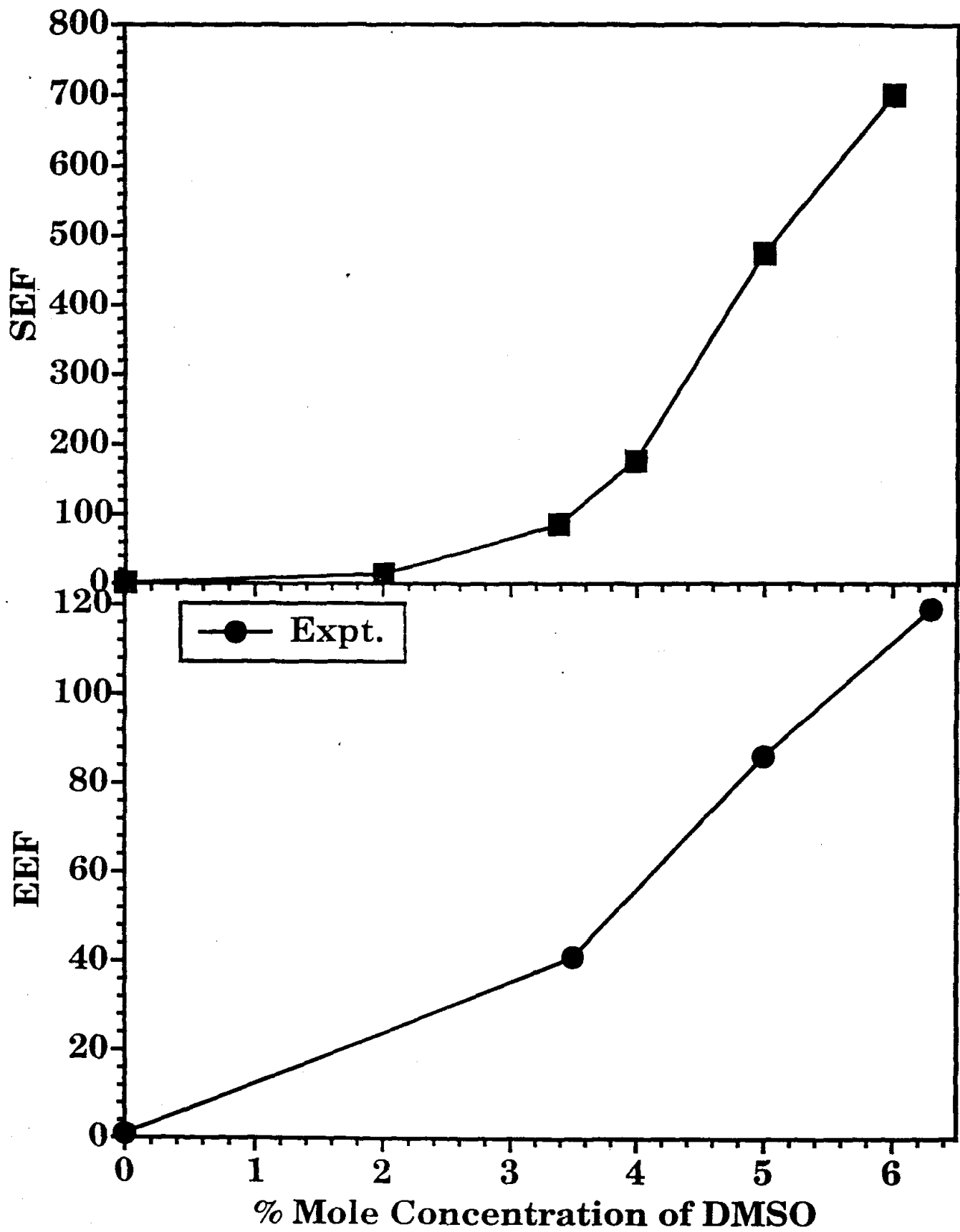
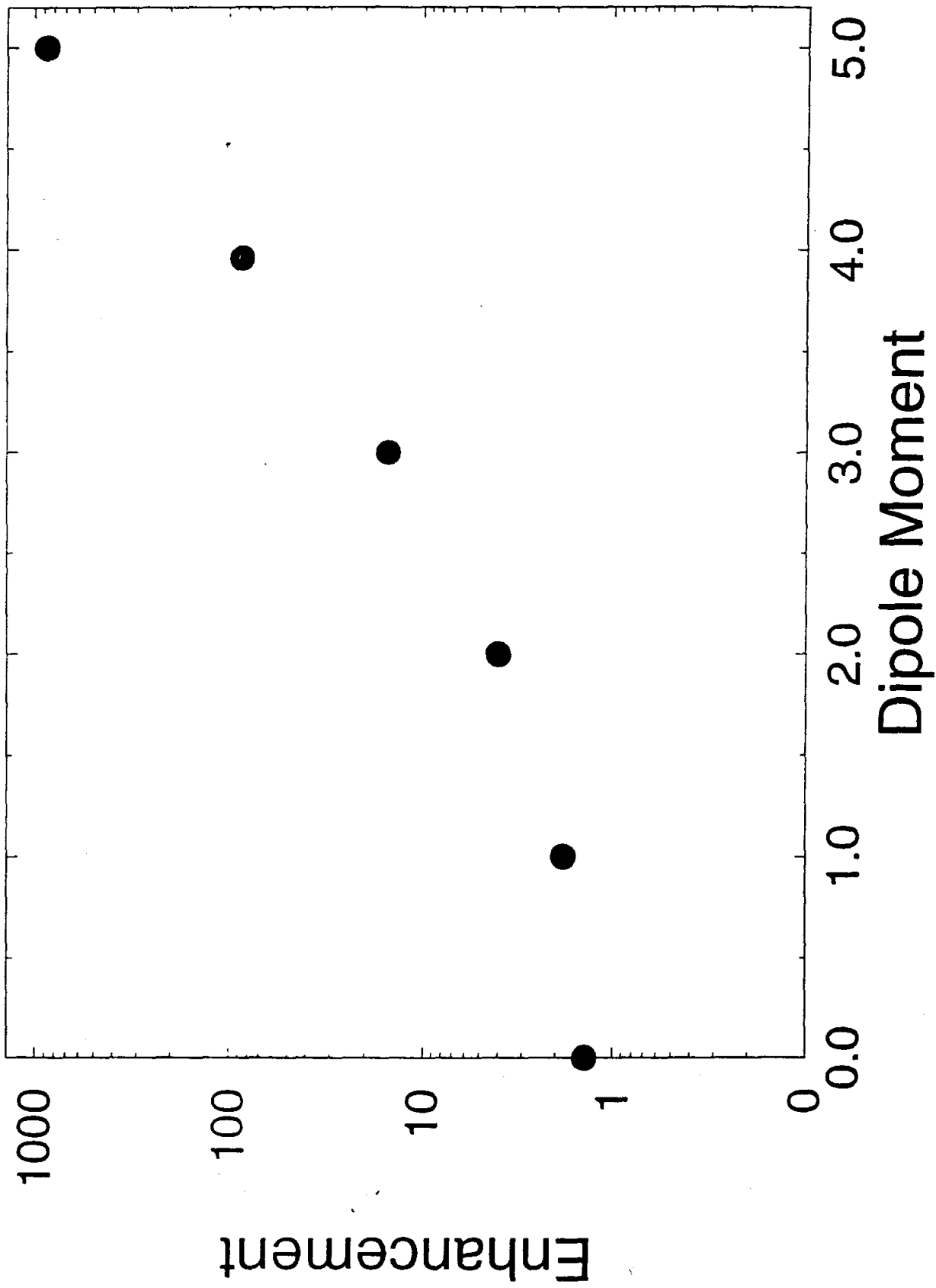
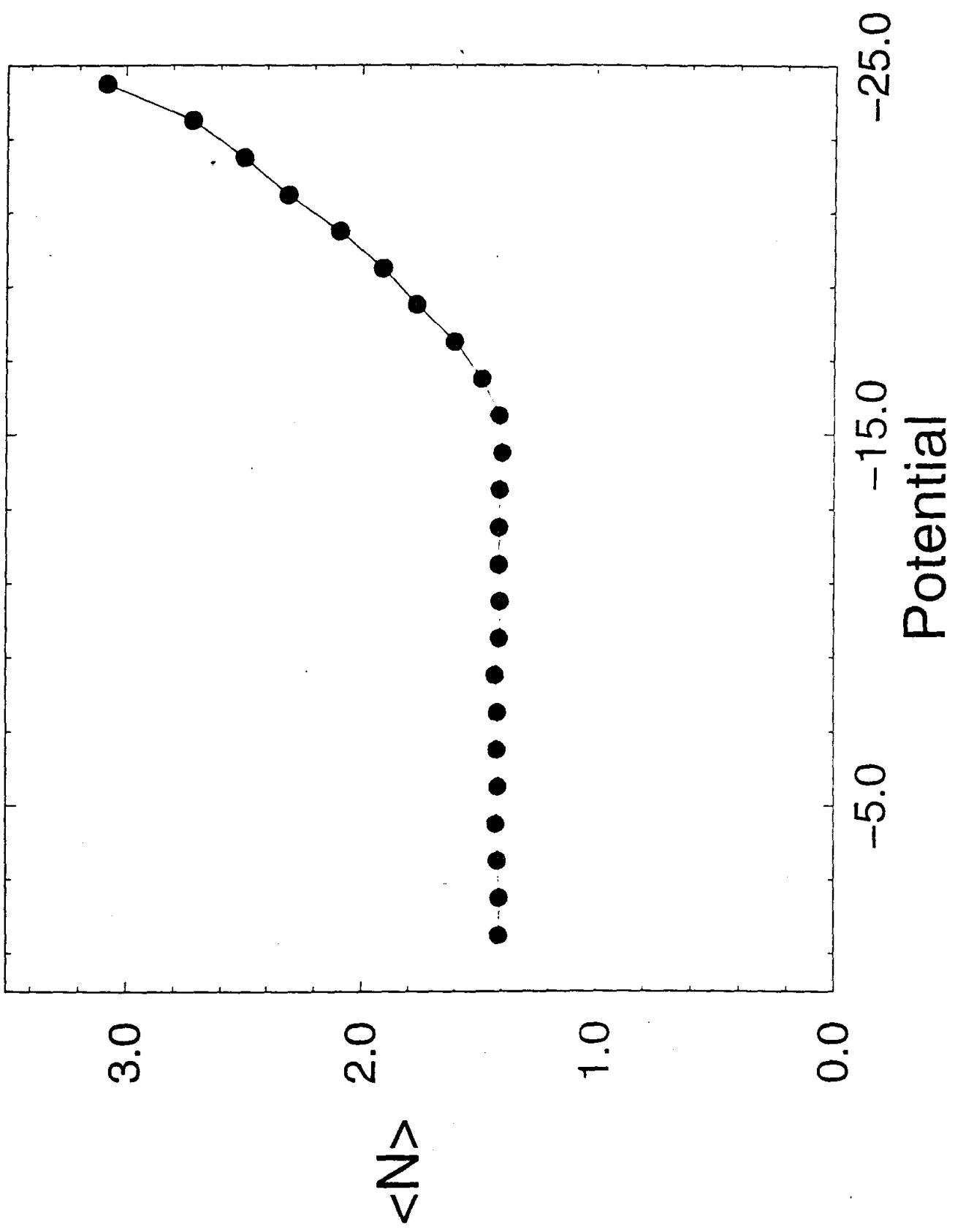


Fig. 1





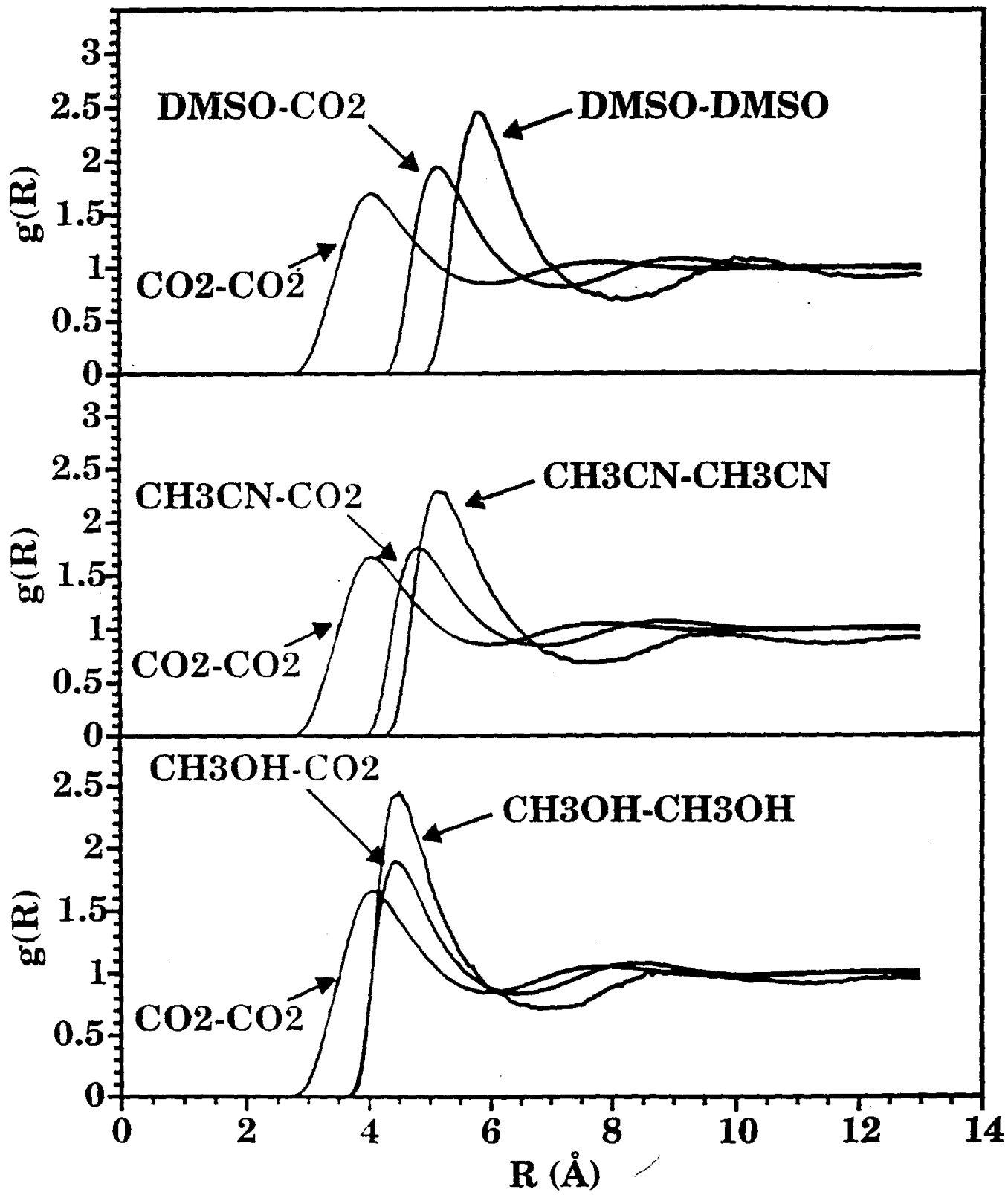


Fig 4

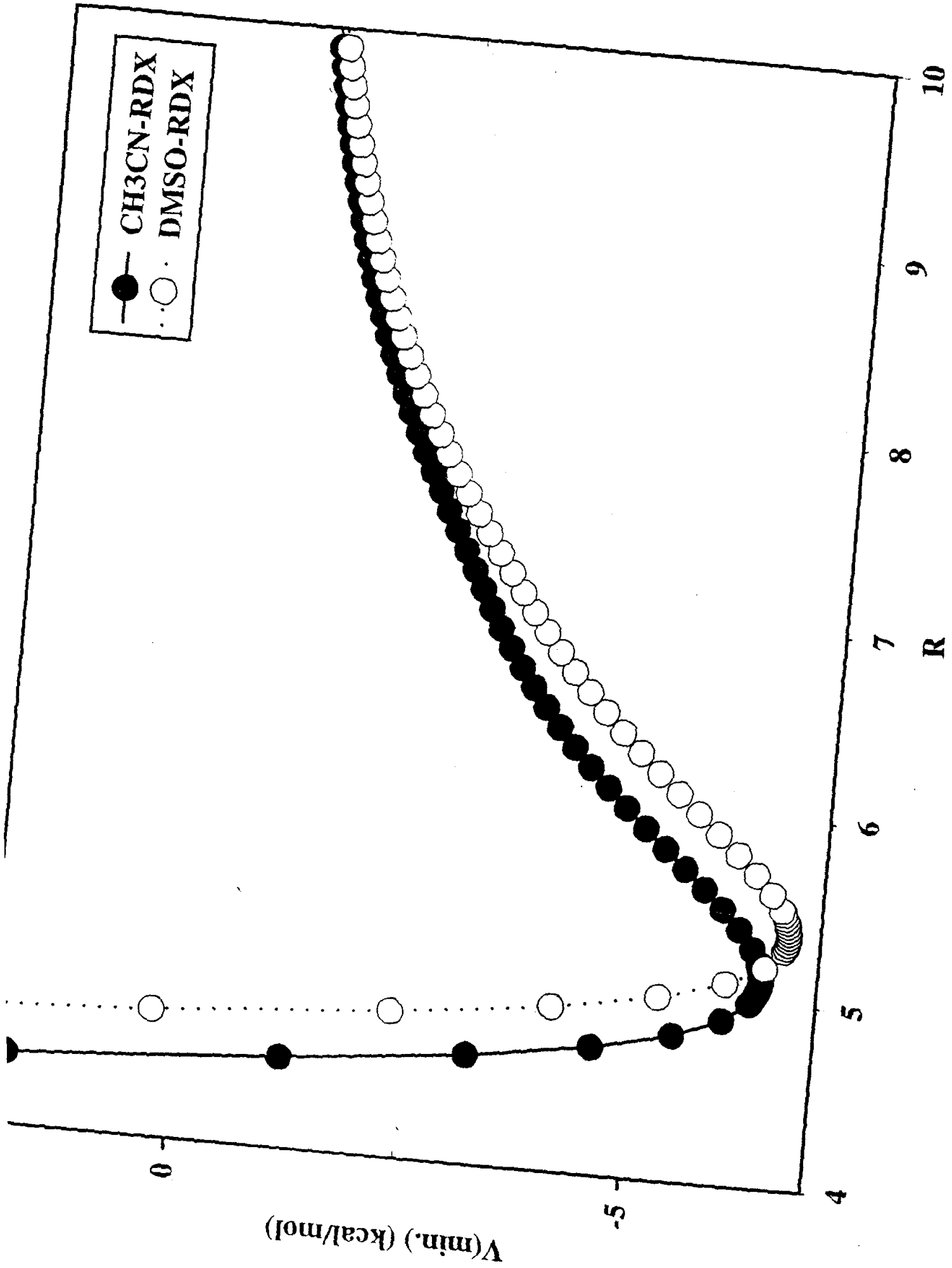


Fig. 5

APPENDIX A
TECHNICAL PUBLICATIONS PRODUCED UNDER PP-695

Open Literature Publications

D. C. Sorescu, B. M. Rice and D. L. Thompson, "Intermolecular Potential for the Hexahydro-1,3,5-trinitro-1,3,5-s-triazine Crystal (RDX): A Crystal Packing, Monte Carlo and Molecular Dynamics Study", *Journal of Physical Chemistry B*, Vol. 101, 798 (1997).

B. M. Rice and C. F. Chabalowski, "*Ab Initio* and Nonlocal Density Functional Study of 1,3,5-trinitro-s-triazine (RDX) Conformers", *Journal of Physical Chemistry A*, Vol. 101, 8720 (1997).

D. C. Sorescu, B. M. Rice and D. L. Thompson, "Molecular Packing and NPT-Molecular Dynamics Investigation of the Transferability of the RDX Intermolecular Potential to 2,4,6,8,10,12-Hexanitrohexaazaisowurtzitane", *Journal of Physical Chemistry B*, Vol. 102, 948 (1998).

D. C. Sorescu, B. M. Rice and D. L. Thompson, "Isothermal-Isobaric Molecular Dynamics Simulations of 1,3,5,7-Tetranitro-1,3,5,7-tetraazacyclooctane (HMX) Crystals", *Journal of Physical Chemistry B*, Vol. 102, 6692 (1998).

H. L. Williams, B. M. Rice and C. F. Chabalowski, "Investigation of the CH₃CN-CO₂ Potential Energy Surface using Symmetry-Adapted Perturbation Theory", *Journal of Physical Chemistry A*, Vol. 102, 6981 (1998).

D. C. Sorescu, B. M. Rice and D. L. Thompson, "A Transferable Intermolecular Potential for Nitramine Crystals", *Journal of Physical Chemistry, A*, Vol. 102, 8386 (1998).

R. Bukowski, J. Sadlej, B. Jeziorski, P. Jankowski, K. Szalewicz, S. Kucharski, H. L. Williams and B. M. Rice, "Intermolecular Potential of Carbon Dioxide Dimer from Symmetry-Adapted Perturbation Theory", *Journal of Chemical Physics*, Vol. 110, p. 3785 (1999).

P. M. Agrawal, D. C. Sorescu, B. M. Rice and D. L. Thompson, "A Model for Predicting the Solubility of RDX in Supercritical CO₂: Isothermal-Isobaric Monte Carlo Simulations", *Fluid Phase Equilibria*, Vol. 155, p. 177 (1999).

D. C. Sorescu, B. M. Rice and D. L. Thompson, "Molecular Packing and Molecular Dynamics Study of the Transferability of a Generalized Nitramine Intermolecular Potential to Non-Nitramine Crystals", *Journal of Physical Chemistry A* Vol. 103, p 989 (1999).

D. C. Sorescu, B. M. Rice and D. L. Thompson, "Theoretical Studies of the Hydrostatic Compression of RDX, HMX, HNIW and PETN Crystals", *Journal of Physical Chemistry*, Vol 103, p. 6783 (1999).

P. M. Agrawal, B. M. Rice, D. C. Sorescu, and D. L. Thompson, "NPT-MC Simulations of Enhanced Solubility of RDX in Polar-Modified Supercritical CO₂", Fluid Phase Equilibria, accepted for publication, in press.

R. Bukowski, K. Szalewicz, and C. F. Chabalowski, "Ab Initio Interaction Potentials for Simulations of Dimethylnitramine Solutions in Supercritical Carbon Dioxide with Cosolvents", Journal of Physical Chemistry A, Vol. 103, 7322 (1999).

ARL Technical Reports

D. C. Sorescu, B. M. Rice and D. L. Thompson, "Intermolecular Potential for the Hexahydro-1,3,5-trinitro-1,3,5-s-triazine Crystal (RDX): A Crystal Packing, Monte Carlo and Molecular Dynamics Study", ARL-TR-1358, May, 1997.

B. M. Rice and C. F. Chabalowski, "Ab Initio and Nonlocal Density Functional Study of 1,3,5-trinitro-s-triazine (RDX) Conformers", ARL-TR-1586, January, 1998.

D. C. Sorescu, B. M. Rice and D. L. Thompson, "Molecular Packing and NPT-Molecular Dynamics Investigation of the Transferability of the RDX Intermolecular Potential to 2,4,6,8,10,12-Hexanitrohexaazaisowurtzitane", ARL-TR-1657, May, 1998.

Awards

"Theoretical Chemistry: An Emerging Practical Tool in Army Research", B. M. Rice, J. Hare, G. Krasko, W. Mattson, S. V. Pai, S. F. Trevino, D. C. Sorescu and D. L. Thompson, Winner of "Best Technical Paper of the Advanced Propulsion and Power Session", 1998 Army Science Conference.